

Supporting Information

Enhanced nonlinear emission from single multilayered metal–dielectric nanocavities resonating in the near-infrared

Nicolò Maccaferri^{1¶}, Attilio Zilli^{2¶}, Tommi Isoniemi^{3,4}, Lavinia Ghirardini², Marzia Iarossi^{4,5},
Marco Finazzi², Michele Celebrano^{2*}, and Francesco De Angelis⁴

¹Department of Physics and Materials Science, University of Luxembourg, L-1511,
Luxembourg, Luxembourg

²Department of Physics, Politecnico di Milano, I-20133, Milano, Italy

³Department of Physics and Astronomy, University of Sheffield, Sheffield S3 7RH, UK

⁴Istituto Italiano di Tecnologia, I-16163, Genova, Italy

⁵Dipartimento di Informatica, Bioingegneria, Robotica e Ingegneria dei Sistemi (DIBRIS),
Università degli Studi di Genova, I-16126 Genova, Italy

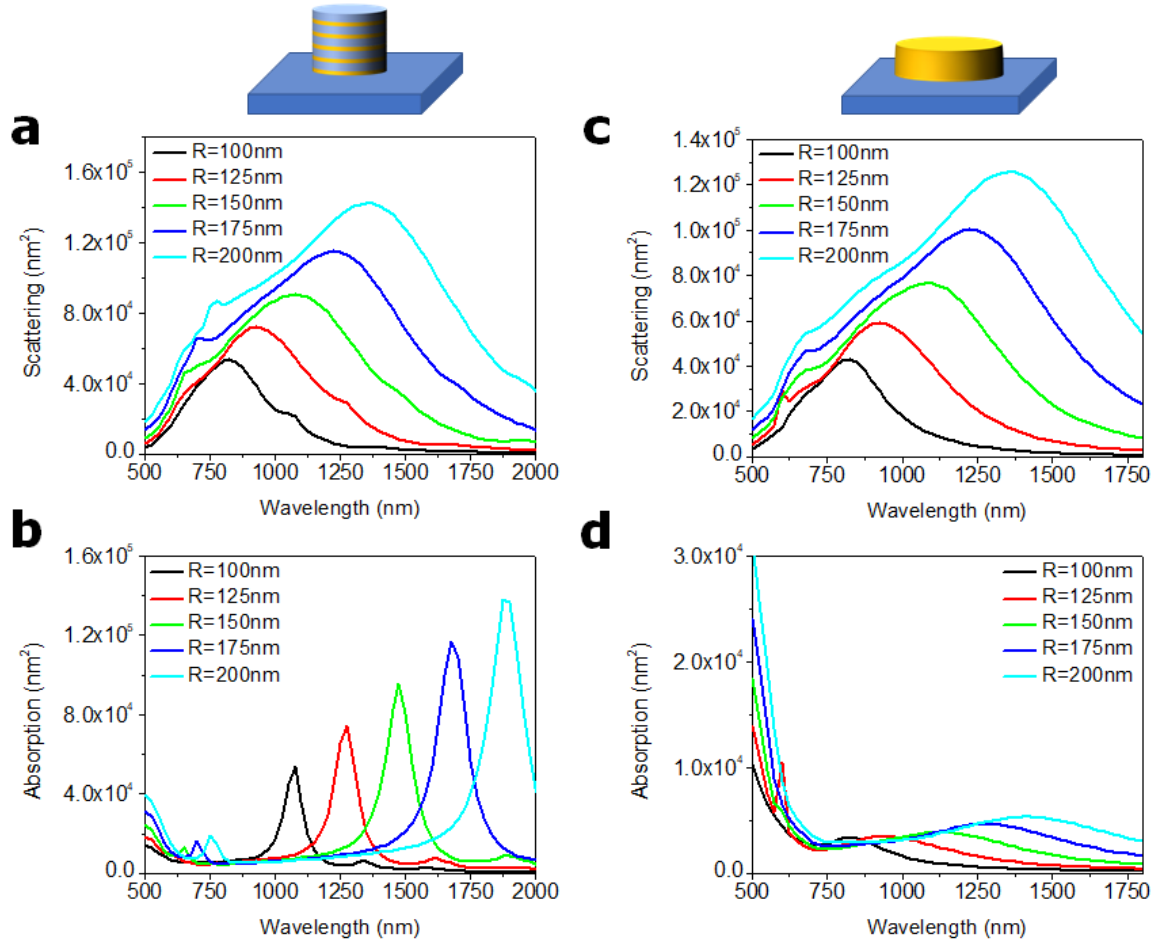


Figure S1. Calculated optical (a) scattering and (b) absorption cross sections of MMD nanostructures with varying radii as a function of the exciting wavelength. Corresponding (c) scattering and (d) absorption cross sections of bulk Au nanoresonators with the same volume of Au as the MMD nanocavities.

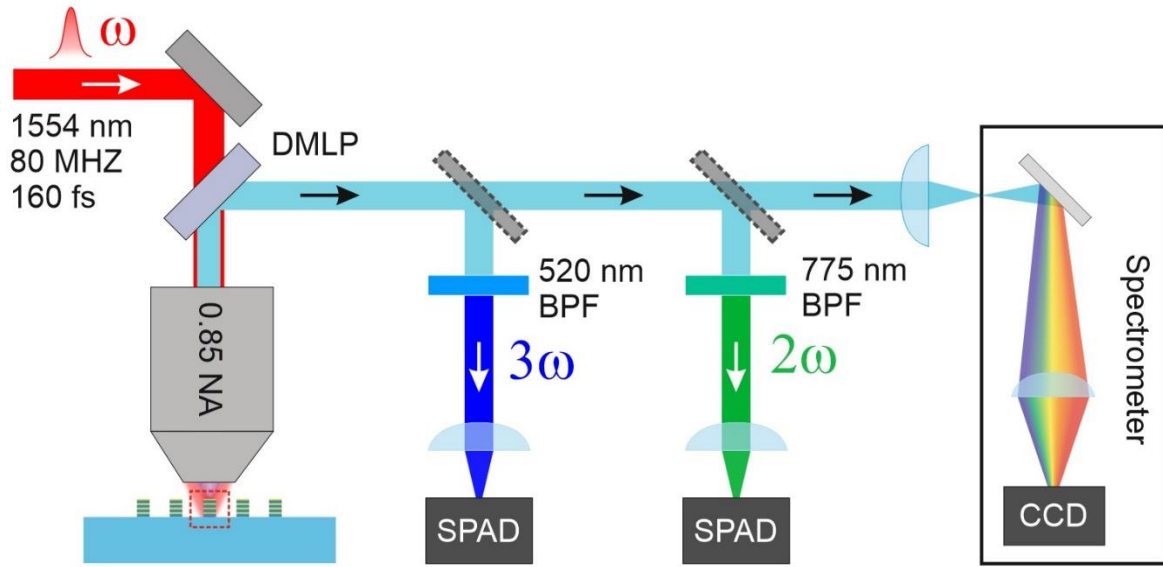


Figure S2. Simplified diagram the nonlinear microscope used in the experiments. Acronyms key: DMLP = dichroic mirror, long pass; BPF = bandpass filter; NA = numerical aperture; SPAD = single-photon avalanche diode; CCD = charge-coupled device.

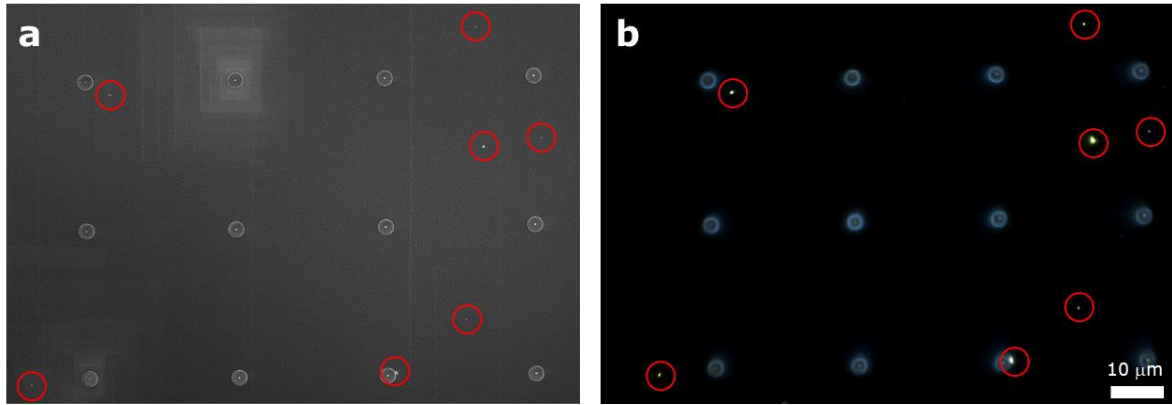


Figure S3. (a) Scanning electron microscopy (SEM) image of a typical region of the MMD sample. (b) Dark field image of the same region. Each row features 4 replicas of a nanocavity with identical radius (from the top: 125 nm, 150 nm, 175 nm). The red circles identify defects on the substrate that act as sources of random SHG in the maps in Figure 1 of the article.

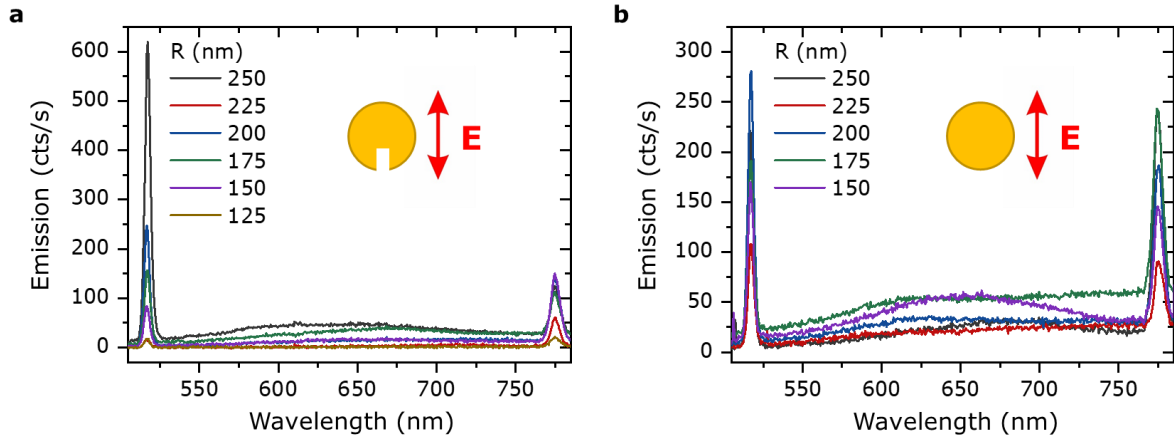


Figure S4. Emission spectra of (a) multilayered “O” nanocavities and (b) multilayered “||” nanocavities of varying radius. As we excite at 1554 nm, SHG and THG occur respectively at 517 nm and 777 nm, corresponding to the position of the two peaks visible in each panel. The broad emission band centered at 650 nm is a multiphoton photoluminescence typical of the X and L bands in gold, see Ref. [1,2].

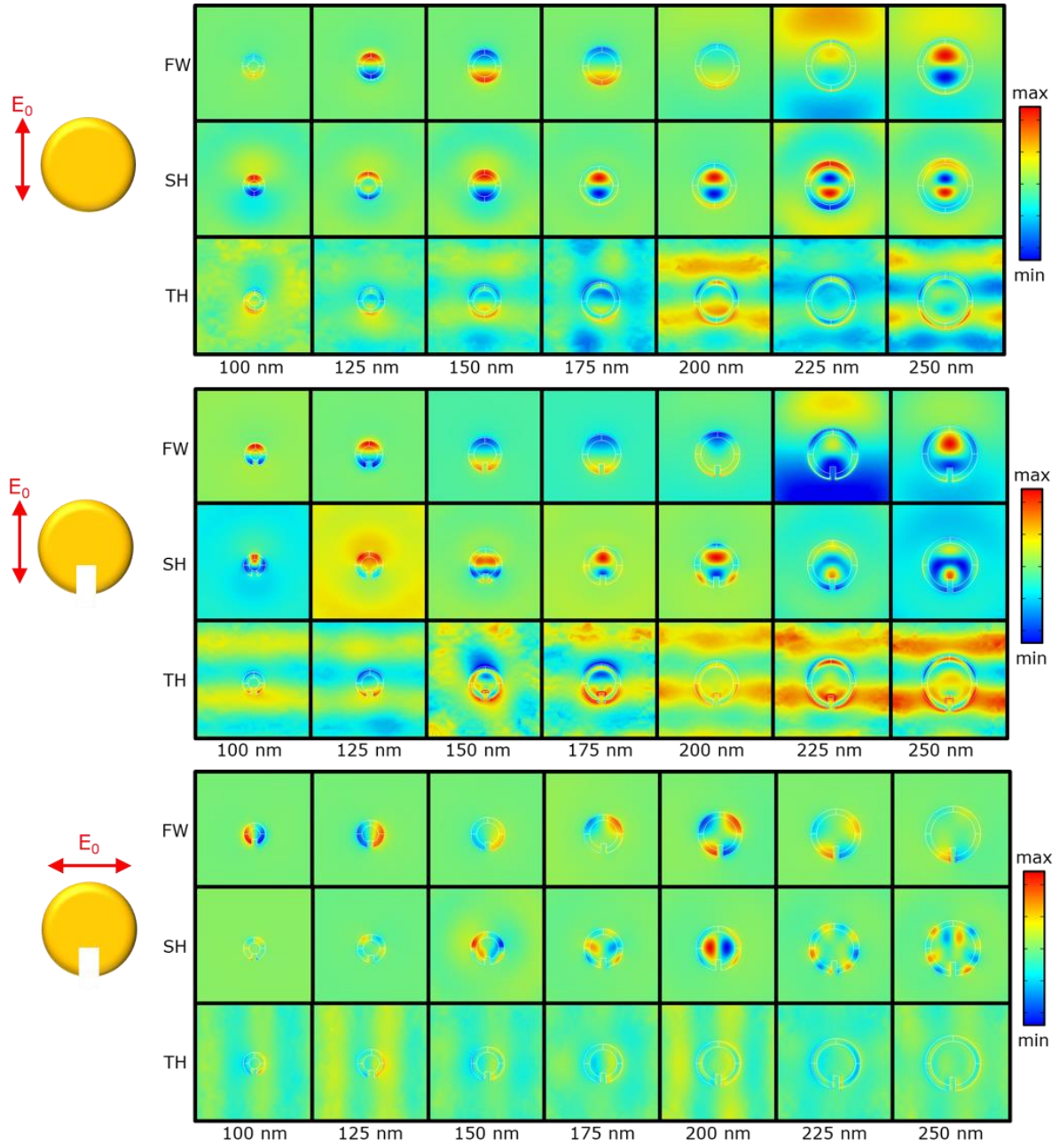


Figure S5. Real part of the z-component of the electric field at the fundamental, SH and TH wavelength for the different MMD nanocavity radii treated in this work.

Supporting Note 1. Estimation of the SHG and THG conversion efficiencies and of the nonlinear coefficients.

Let us estimate the conversion efficiencies $\eta_{\text{SHG}} = \frac{P_{\text{SHG}}^{\text{out}}}{P_{\text{FW}}^{\text{in}}}$ and $\eta_{\text{THG}} = \frac{P_{\text{THG}}^{\text{out}}}{P_{\text{FW}}^{\text{in}}}$, where $P_{\text{FW}}^{\text{in}} = 500 \mu\text{W}$ is the average pump power used in experiments (peak fluence $1 \text{ GW}/\text{cm}^2$). We estimate as follows the optical throughput of our setup for the SHG (THG) signal. The light emitted by the nanoparticle within the solid angle of detection of the objective is 70% (70%) of the total, since we collect from the higher refractive index half-space. The light transmitted by the microscope objective is 85% (95%), while the metallic mirrors and the dichroic mirror reflects 96% (96%) and 99%, (99%) respectively. The quantum efficiency of the SPAD is 15% (45%) at 777 nm (518 nm), while the light effectively collected by the SPAD (filling factor) is 50% (80%), due to the finite size of the device ($50 \mu\text{m}$). Therefore, the overall optical throughput is 4% (20%).

Based on this estimate, the most efficient MMD antenna emits $4 \times 10^4 / 0.04 = 1 \times 10^6$ photons/s, which corresponds to an average power of about 300 fW at 777 nm. Hence, we obtain a conversion efficiency $\eta_{\text{SHG}} = \frac{P_{\text{SHG}}^{\text{out}}}{P_{\text{FW}}^{\text{in}}} \cong 6 \times 10^{-10}$, whereas for the bulk gold structures η_{SHG} is of the order 10^{-11} . Similarly, the highest THG signal measured is $5 \times 10^4 / 0.22 = 2.3 \times 10^5$ photons/s, corresponding to a conversion efficiency $\eta_{\text{THG}} = \frac{P_{\text{THG}}^{\text{out}}}{P_{\text{FW}}^{\text{in}}} \cong 1.8 \times 10^{-10}$.

Some different, and perhaps more telling, figures of merit, are the nonlinear coefficients $\gamma_{\text{SHG}} = \frac{\hat{P}_{\text{SHG}}^{\text{out}}}{(\hat{P}_{\text{FW}}^{\text{in}})^2}$ and $\gamma_{\text{THG}} = \frac{\hat{P}_{\text{THG}}^{\text{out}}}{(\hat{P}_{\text{FW}}^{\text{in}})^3}$, obtained by dividing the peak powers () of the emitted nonlinear signal $\hat{P}_{\text{SHG}}^{\text{out}}$ ($\hat{P}_{\text{THG}}^{\text{out}}$) by the square $(\hat{P}_{\text{FW}}^{\text{in}})^2$ and the cube $(\hat{P}_{\text{FW}}^{\text{in}})^3$ of the impinging powers respectively, where $\hat{P} = P / f_{\text{rep}} \Delta \tau_{\text{pulse}}$. In fact, these coefficients are independent from both the repetition rate, f_{rep} , and pulse width, $\Delta \tau_{\text{pulse}}$, of the excitation pulses. In our case these numbers are respectively $\gamma_{\text{SHG}} \cong 10^{-11} \text{ W}^{-1}$ and $\gamma_{\text{THG}} \cong 10^{-13} \text{ W}^{-2}$.

Finally, we shall derive the *effective* nonlinear susceptibilities $\chi_{\text{eff}}^{(2)}$ and $\chi_{\text{eff}}^{(3)}$, which give an absolute description of the nonlinear performance of the nanocavity independently from the experimental configuration, but do not correspond to the local $\chi_{\text{eff}}^{(n)}$ of the materials since they do not account for the inhomogeneous distribution of the nonlinear sources both in the volume and at the surface of the nanocavity. In this case, following Ref. [3], we obtain:

$$\chi_{\text{eff}}^{(2)} = \sqrt{\hat{\gamma}_{\text{SHG}} \frac{3\pi\epsilon_0 c A_{\text{eff}}^2}{k^4 V^2}} \cong 1.5 \text{ pm V}^{-1},$$

and

$$\chi_{\text{eff}}^{(3)} = \sqrt{\hat{\gamma}_{\text{THG}} \frac{1.5\pi\epsilon_0^2 c^2 A_{\text{eff}}^3}{k^4 V^2}} \cong 1.1 \times 10^{-20} \text{ m}^2 \text{ V}^{-2}.$$

where $A_{\text{eff}} = \pi \times (0.67 \times 1554 \text{ nm}/0.85)^2 = 4.7 \times 10^{-12} \text{ m}^2$ is the area of the diffraction-limited pump and $V = \pi \times (200 \text{ nm})^2 \times 400 \text{ nm} = 5.0 \times 10^{-20} \text{ m}^3$ is the volume of the most resonant structures.

-
- [1] Bouhelier, A.; Bachelot, R.; Lerondel, G.; Kostcheev, S.; Royer, P.; Wiederrecht, G. P. Surface Plasmon Characteristics of Tunable Photoluminescence in Single Gold Nanorods. *Phys. Rev. Lett.* **2005**, *95*, 267405.
- [2] Bouhelier, A.; Beversluis, M. R.; Novotny L. Characterization of nanoplasmonic structures by locally excited photoluminescence. *Appl. Phys. Lett.* **2003**, *83*, 5041.
- [3] Hsieh, C.-L.; Pu, Y.; Grange, R.; Psaltis, D. Second harmonic generation from nanocrystals under linearly and circularly polarized excitations. *Opt. Express* **2010**, *18*, 11917.